SPHERICAL SHELL MODEL OF AN ASYMMETRIC R.F. DISCHARGE

by

M. A. Lieberman

Memorandum No. UCB/ERL M88/65

25 October 1988

SPHERICAL SHELL MODEL OF AN ASYMMETRIC R.F. DISCHARGE

by

M. A. Lieberman

Memorandum No. UCB/ERL M88/65

25 October 1988

ELECTRONICS RESEARCH LABORATORY

College of Engineering
University of California, Berkeley
94720

TITLE PAGE

SPHERICAL SHELL MODEL OF AN ASYMMETRIC R.F. DISCHARGE

by

M. A. Lieberman

Memorandum No. UCB/ERL M88/65

25 October 1988

ELECTRONICS RESEARCH LABORATORY

College of Engineering
University of California, Berkeley
94720

SPHERICAL SHELL MODEL OF AN ASYMMETRIC R.F. DISCHARGE

M. A. LIEBERMAN

Department of Electrical Engineering and Computer Sciences

and the Electronics Research Laboratory

University of California, Berkeley, CA 94720

ABSTRACT

A spherical shell model is used to study ion transport and bias voltage formation in asymmetric, capacitive r.f. discharges, which have unequal areas A and glow-to-electrode voltages V at the powered (a) and grounded (b) electrodes. Ions are generated by thermal electron ionization and are lost by ambipolar diffusion in the glow. Resonant charge transfer with a constant cross section is assumed to dominate the ion transport. We obtain the density ratio scaling $n_a/n_b \propto (A_b/A_a)^{7/24}$, where n is the density at the glow-sheath edge. Three electrode sheath models are considered: collisionless (Child's law), collisional (Cobine's law), and a constant cross section collisional law. Using these and the continuity of the r.f. current flow, we obtain the scaling of the electrode voltage ratio with the electrode area ratio: $V_a/V_b \propto (A_b/A_a)^q$. For typical r.f. materials processing discharges, the constant cross section law yields $q \approx 2.21$. The effects of secondary electron ionization and local ionization near the sheaths due to stochastic heating are shown to further reduce the value of q.

I. INTRODUCTION

Capacitive, radio frequency (r.f.) discharges are widely used for materials processing in the electronics industry. Typical discharge parameters are pressure $p \approx$ 10–300 mTorr, $\omega/2\pi \approx$ 13.56 MHz, voltage $V_{rf} \approx$ 50-1000 V, and electrode spacing $l \approx$ 3–10 cm. The discharges are generally asymmetric; ie, the r.f. powered electrode a and the grounded electrode b have different areas, with A_a typically less than A_b. Although many phenomena occurring in these discharges have been studied during the last years[1–16], there have been few studies of the discharge asymmetry. This asymmetry determines the magnitude of the self-bias voltage V_a (the ion bombarding energy) at the powered electrode, which is a critical parameter for VLSI processing. A simple collisionless discharge model[1] yields the scaling $V_a/V_b = (A_b/A_a)^4$, contrary to measurements[1–2,15–16] that indicate a much weaker dependence of V_a/V_b on the area ratio.

For capacitive discharges, almost all the applied r.f. voltage is dropped across thin sheaths, having thicknesses s_a and s_b, at the powered and grounded electrodes. In the pressure regime of interest, the ion-neutral mean free path λ_i is short compared to s_a and s_b. For example, in an argon discharge $\lambda_i \approx (200p)^{-1}$ cm; for $s \approx 1$ cm, we obtain $\lambda_i \lesssim s$ for $p \gtrsim 5$ mTorr. It follows that the assumption of Child law scaling[17] for the ion current density, $J \propto V^{3/2}/s^2$, is usually not valid. Cobine[18] gives the scaling $J \propto V^2/s^3$ for constant ion mobility (constant ion mean free time τ_i. However, the collisional ion process that dominates the ion transport is charge transfer of the ion with the parent neutral gas. This resonant process has a cross section, and therefore a mean free path, that is roughly a constant, independent of the ion drift velocity u. Because u varies within the sheath, $\tau_i \approx \lambda_i/u$ is not a constant.

A thermal plasma or "glow" region between the sheaths having a thickness $d \gtrsim s$ serves to maintain the discharge by means of the balance between ion generation there and loss to the electrodes. For low pressures, the electron temperature T_e in the glow is uniform, and the volume ionization rate is $\nu_{iz} n$, where ν_{iz} is the ionization frequency and n is the electron density. Secondary electrons and local ionization near the sheaths can also contribute to the ionization. Ions are lost by ambipolar diffusion to the two electrodes. For a constant λ_i, the diffusion coefficient is not a constant, but is inversely proportional to u, which varies within the glow. These processes of ionization and diffusion determine the plasma density profile and, in particular, the densities at the two sheath edges near the powered and grounded electrodes, which are not equal as is so often assumed. In turn, these densities determine the sheath properties and thus the sheath voltages V_a and V_b. Godyak and collaborators[19] have developed and solved the ion transport equations in the glow for a *symmetric* discharge (equal areas for the powered and grounded electrodes) for these processes.

In this work we develop a simple spherical shell model to determine the sheath scaling law and the density profile in the thermal plasma in an asymmetric discharge. We consider the short mean free path regime $\lambda_i \leq s, d$ and first treat the case of thermal electron ionization in the glow. After finding the scaling law for the ratio of the densities at the sheath edges in terms of the ratio of the electrode areas, we determine the ratio of the self-bias voltages at the electrodes. We then consider the additional effects of secondary electron ionization in the glow and local ionization near the sheaths. Savas[20-21] has developed a numerical model of an asymmetric discharge using spherical shell electrodes. We compare our results to these numerical code results, which include some effects not present in the simple model.

II. TRANSPORT MODEL IN THE GLOW

We introduce the spherical shell model shown in Fig. 1. The powered electrode is the inner sphere a having radius r_a, and the grounded electrode is the outer sphere b having radius r_b. The electrode separation l, plasma thickness d, and sheath thicknesses s_a and s_b are defined in the figure. The discharge is driven by an r.f. current source through a blocking capacitor C_B having negligible impedance at the r.f. driving frequency. Since the system is spherically symmetric, the model is purely one-dimensional (along r). The freedom to choose not only the plasma length $d = r_a - r_b$ but also the powered-to-grounded electrode *area ratio* $\beta^2 = r_a^2/r_b^2 < 1$ allows us to model an asymmetric discharge.

The assumptions for the transport model are:

(1) The ion temperature $T_i \ll T_e$ and the ion thermal velocity $u_{Ti} \ll u$, the ion drift velocity due to the ambipolar electric field within the glow.

(2) The dominant ion collisional process is charge exchange of the ion with the parent neutral gas atom. The cross section σ_i and, consequently, the mean free path $\lambda_i = (n_0\sigma_i)^{-1}$ for this process is a constant, independent of ion energy.

Since the transport process is assumed to be ambipolar diffusion, the ion and electron particle fluxes in the glow are given by

$$\Gamma_i = \mu_i (nE - T_i \frac{dn}{dr}) , \tag{1}$$

$$\Gamma_e = \mu_e (-nE - T_e \frac{dn}{dr}) , \tag{2}$$

where μ_i and μ_e are the ion and electron mobilities, $n(r)$ is the plasma density, and E is the ambipolar electric field. Since the transport is ambipolar, $\Gamma_i = \Gamma_e = \Gamma$. Because $T_i \ll T_e$ and $\mu_i \ll \mu_e$, we obtain from (1) that

$$\Gamma = nu = \mu_i nE \tag{3}$$

and from (2) that

$$\frac{dn}{dr} = -nE/T_e , \tag{4}$$

where

$$\mu_i = \frac{e}{M\,|u|} \frac{2}{\pi} \lambda_i . \tag{5}$$

The factor of $2/\pi$ in (5) accounts for the time averaging of the ion velocity over the distribution of mean free paths to obtain the mean velocity u. The inverse dependence of μ_i on $|u|$ arises because by assumption (2) $u_{Ti} \ll |u|$; if this ordering is reversed, than $|u|$ in (5) should be replaced by u_{Ti}. This is indeed the case near the radius r within the glow where u passes through zero. We assume that the region over which $u_{Ti} \gg |u|$ is small compared to d. Using (3) and (5), we obtain

$$E = \frac{\pi M}{2e\lambda_i} u\,|u| . \tag{6}$$

III. THERMAL ELECTRON IONIZATION

We assume that the electron temperature T_e within the glow is uniform and constant, such that the ionization frequency ν_{iz} is a function of T_e and the neutral gas density n_0 alone. This assumption typically is valid for pressures below 100 mTorr. The particle conservation law within the glow can be written

$$\nabla \cdot \Gamma = \frac{1}{r^2}\frac{d}{dr}(r^2 nu) = \nu_{iz} n \ . \tag{7}$$

Expanding the derivative in (7) and substituting for dn/dr using (4) and E using (6), we obtain

$$\frac{du}{dr} - \alpha u^2 |u| + \frac{2u}{r} = \nu_{iz} \ , \tag{8}$$

where

$$\alpha = \frac{\pi M}{2e\lambda_i T_e} \ . \tag{9}$$

Equation (8) is a first order nonlinear differential equation to determine the ambipolar drift velocity u. We choose the usual boundary conditions at the plasma sheath edges that $u(r_a) = -u_B$ and that $u(r_b) = u_B$, where $u_B = (eT_e/M)^{1/2}$ is the Bohm (ion sound) velocity.

The density profile corresponding to a given solution $u(r)$ of (8) is obtained by substituting (6) into (4), yielding the equation

$$\frac{1}{n}\frac{dn}{dr} = -\alpha u \ |u| \ , \tag{10}$$

which is integrated to determine n.

We introduce normalized variables $U = u/u_B$, $R = r/(2\lambda_i/\pi)$, and $N = n/n(r_a)$. Then (8) and (10) can be written as

$$\frac{dU}{dR} + \frac{2U}{R} = U^2 |U| + \varepsilon \ , \tag{11}$$

$$\frac{dN}{dR} = -N\, U\, |U| \ , \tag{12}$$

where

$$\varepsilon = \frac{2}{\pi}\frac{\lambda_i}{u_B}\nu_{iz} \ . \tag{13}$$

The boundary conditions are that $U = -1$ at $R = R_a$, $U = +1$ at $R = R_b$, and that $N = 1$ at $R = R_a$.

The procedure for integrating (11) and (12) is as follows: We choose $U = -1$ and $N = 1$ at some value of R_a and integrate both equations until we reach the value $U = 1$. At this point we have obtained R_b as well as the dependence of N on R. We use a Runge-Kutta integration scheme.

The results of the integration are as follows: We find that the difference $D = R_b - R_a$ is practically independent of R_a, and is a function of ε alone. These results are shown in Fig. 2. A good fit to the data over the range $.01 < \varepsilon < 0.3$ and $.05 < \beta^2 < 0.9$ is $D \approx 2.05\,\varepsilon^{-.702}$. Unnormalizing this expression for D and solving for ν_{iz}, we obtain

$$\nu_{iz}\, d \approx 2.3\, u_B (\lambda_i / d)^{.42} \ . \tag{14}$$

For a specified value of pd, (14) determines the electron temperature T_e of the glow. Godyak[19] gives an approximate expression

$$\nu_{iz}\, d \approx 2\sqrt{2}\, u_B (\lambda_i / d)^{1/2} \tag{15}$$

for the symmetric case, which is close to that given by (14). Godyak's dependence is shown in Fig. 2 as the dashed line.

The density N rises from $N_a = 1$ at R_a to N_{max} as R increases, and then falls to N_b at R_b. Figure 3 shows the dependence of the various density ratios n_{max}/n_a, n_{max}/n_b and n_b/n_a on $\beta^{-1} = r_b/r_a$ and ε.

Godyak[19] has obtained the expression

$$\frac{n_{max}}{n_a} = \frac{n_{max}}{n_b} = \left[\frac{1}{\varepsilon} + 1\right]^{1/3} \tag{16}$$

for the symmetric case $\beta = 1$. We find that a good fit to the data of Fig. 3 is

$$\frac{n_{max}}{n_a} \approx \left[\frac{\beta}{\varepsilon} + 1\right]^{1/3} \tag{17}$$

and

$$\frac{n_{\max}}{n_b} \approx \left[\frac{1}{\varepsilon\beta^{3/4}} + 1 \right]^{1/3} . \tag{18}$$

Consequently, we obtain

$$\frac{n_b}{n_a} \approx \left[\frac{\beta}{\varepsilon} + 1 \right]^{1/3} \left[\frac{1}{\varepsilon\beta^{3/4}} + 1 \right]^{-1/3} . \tag{19}$$

For the usual case $\varepsilon\beta^{3/4} \ll 1$, we obtain the simple expression for the ratio of densities at the grounded and powered electrodes:

$$\frac{n_b}{n_a} \approx \beta^{7/12} = \left[\frac{A_a}{A_b} \right]^{7/24} , \tag{20}$$

which is independent of ε.

Savas[20-21] has developed a code to determine the ion transport in the glow, including the effects of ion inertia and finite ion temperature. His results[21], which are shown in Fig. 3, are in good agreement with the model results obtained here.

IV. SHEATH MODEL

The sheath properties play a critical role in determining the self-bias voltage at the powered electrode. Since generally $s \ll r_a$, we can use rectangular geometry to obtain the sheath scaling law, letting $x = 0$ at the plasma-sheath edge and $x = s$ at the electrode. The usual assumption is collisionless ion flow within the sheath, which leads to Child's law[17]

$$J = \frac{4}{9}\varepsilon_0 \left[\frac{2e}{M} \right]^{1/2} \frac{V^{3/2}}{s^2} , \tag{21}$$

where $J = en_s u_B$ is the ion current density, with n_s the ion density at the plasma-sheath edge. Equation (21) does not include the self-consistent effect of the time-average electron space charge within the sheath. Lieberman[22] includes this effect to obtain (21) with 4/9 replaced by 200/243. However, we have noted that (21) is valid only at very low pressures.

Cobine[18] assumes collisional ion flow with a constant ion mobility μ_i (constant ion mean free time) within the sheath, obtaining

$$J = \frac{9}{8}\varepsilon_0\mu_i\frac{V^2}{s^3} . \tag{22}$$

However, (22) is valid only at very high pressures (low drift velocities), such that $u \lesssim u_{Ti}$.

In the intermediate pressure regime of interest, for which $\lambda_i \approx$ const, the appropriate sheath law is found as follows: We let

$$u = \mu_i E \tag{23}$$

in the sheath, where μ_i is given by (5). Since the ion flux is conserved in the sheath,

$$nu = n_s u_B . \tag{24}$$

Letting $E = -d\Phi/dx$, where Φ is the potential in the sheath, we obtain using (5) and (23) that

$$u^2 = -\frac{2e\lambda_i}{\pi M}\frac{d\Phi}{dx} . \tag{25}$$

Poisson's equation in the sheath is

$$\frac{d^2\Phi}{dx^2} = -\frac{en}{\varepsilon_0} . \tag{26}$$

Differentiating (25) and using (24) and (26), we obtain

$$\frac{d\,(u^2)}{dx^2} = \frac{2u_B^3\lambda_i}{\pi\lambda_D^2 u} , \tag{27}$$

where $\lambda_D = (\varepsilon_0 T_e/en_s)^{1/2}$ is the Debye length at the plasma-sheath edge. Integrating (27) and using the condition that $u = u_B$ at $x = 0$, we obtain

$$u = u_B\left[1 + \frac{3}{\pi}\frac{\lambda_i x}{\lambda_D^2}\right]^{1/3} . \tag{28}$$

Inserting (28) into (25) and integrating, we obtain

$$\Phi = -\frac{\pi^2}{10}\left[\frac{\lambda_D}{\lambda_i}\right]^2 T_e\left[\left[1 + \frac{3}{\pi}\frac{\lambda_i x}{\lambda_D^2}\right]^{5/3} - 1\right] , \tag{29}$$

where we have chosen $\Phi = 0$ at $x = 0$. Letting $\Phi = -V$ at $x = s$ and assuming that $\lambda_i s \gg \lambda_D^2$, we obtain

$$\frac{1}{\lambda_D^2} = \left[\frac{1000}{243\pi}\right]^{1/2} \left[\frac{V}{T_e}\right]^{3/2} \frac{\lambda_i^{1/2}}{s^{5/2}} . \tag{30}$$

Substituting for λ_D in terms of n_s and T_e and using $n_s = J/eu_B$, we obtain the sheath law

$$J = \left[\frac{500}{243\pi}\right]^{1/2} \varepsilon_0 \left[\frac{2e}{M}\right]^{1/2} \frac{V^{3/2}\lambda_i^{1/2}}{s^{5/2}} . \tag{31}$$

If we include the effect of the self-consistent electron space charge within the sheath[23], then we obtain (31) with $(500/243\pi)^{1/2}$ replaced by 2.10. Equation (31) is a reasonable choice for the sheath scaling law in the pressure regime of interest for materials processing discharges.

V. ELECTRODE BIAS VOLTAGE

The scaling of the electrode bias voltages with discharge asymmetry is determined by the continuity of r.f. current within the discharge, by the d.c. $J-V-s$ scaling law of each sheath, and by the magnitude of the d.c. ion currents flowing from the plasma across each sheath. We assume that the sheaths are capacitive and that the r.f. voltage amplitude V_{rf} across each sheath is equal to the d.c. glow-to-electrode voltage V across the sheath. The latter assumption holds provided $V_{rf} \gg T_e$ and $\omega \gg \omega_{pi}$, where ω_{pi} is the ion plasma frequency within the sheath.

Since the sheath capacitance is proportional to the ratio of sheath area to sheath thickness, continuity of r.f. current requires

$$V_a A_a / s_a = V_b A_b / s_b . \tag{32}$$

We assume that (31) is the scaling law for each sheath. Using $J_a = en_a u_B$ and $J_b = en_b u_B$ in (31) yields the scaling

$$\frac{n_a s_a^{5/2}}{V_a^{3/2}} = \frac{n_b s_b^{5/2}}{V_b^{3/2}} . \tag{33}$$

Using (32) in (33) to eliminate s, we obtain

$$\frac{n_a}{n_b} = \left[\frac{V_b}{V_a}\right] \left[\frac{A_b}{A_a}\right]^{5/2} . \tag{34}$$

For collisional diffusion with constant λ_i in the glow, we use (20) in (34) to eliminate n_a/n_b. Recalling that $\beta = (A_a/A_b)^{1/2}$, we obtain the scaling law for the ratio of the bias voltages at the powered and grounded electrodes

$$\frac{V_a}{V_b} = \left[\frac{A_b}{A_a}\right]^q , \tag{35}$$

where the area ratio scaling exponent is $q = 53/24 \approx 2.21$. For a homogeneous density in the glow such that $n_a/n_b = 1$, we obtain $q = 5/2$.

If Child's law (21) for the sheaths is used in place of (31), then we obtain $q = 41/12 \approx 3.42$ for collisional diffusion and $q = 4$ for a homogeneous density in the glow. If Cobine's sheath law (22) is used, then $q = 65/24 \approx 2.71$ for collisional diffusion and $q = 3$ for a homogeneous density. These values of the area ratio scaling exponent q are summarized in Table 1. We see that the main factor influencing the scaling exponent is the sheath scaling law, although the ion transport process has a small but significant effect. The scaling exponent is significantly reduced, from $q = 4$ to $q = 2.21$, when ion collisions in the sheath and plasma are properly accounted for.

VI. EFFECT OF SECONDARY ELECTRONS

We consider the effect of secondary electron ionization in the regime for which the secondary electron mean free path $\lambda_{se} \gg l$ and the collision time $\tau_{se} \gg \tau_{sl}$, where $\tau_{sl} \approx \omega^{-1}$ is the lifetime of secondary electrons due to losses at the electrodes[24-25]. At high frequencies (e.g., $f \gtrsim 13.56$ MHz), secondary electron ionization is not as important as ionization due to thermal electrons in the glow; however, as the frequency is reduced it increases in importance. We can understand the effect of this ionization process on the area scaling exponent q by considering that it is the dominant process. Since secondary electrons enter the discharge with high energies ($\sim V_a, V_b$) and are lost before collisionally scattering, the ionization rate is modeled as A/r^2, where A is a constant independent of the radial coordinate r. The particle conservation law within the plasma is

$$\frac{1}{r^2}\frac{d}{dr}(r^2 nu) = \frac{A}{r^2} , \tag{36}$$

which can be integrated to obtain

$$nu = A(r - r_0)/r^2 \,, \tag{37}$$

where the integration constant r_0 specifies the radius at which the flux nu vanishes. Substituting (6) into (4) and multiplying by n, we obtain

$$-\frac{1}{2}\frac{dn^2}{dr} = \pm\alpha(nu)^2 \,, \tag{38}$$

where the upper (lower) sign applies for u greater (less) than zero. Substituting (37) into (38) and integrating, we obtain

$$\frac{n^2 - n_{\max}^2}{2} = \pm\frac{\alpha A^2}{3r_0}\left[\frac{r_0}{r} - 1\right]^3 , \tag{39}$$

where we have chosen $n = n_{\max}$ at $r = r_0$.

We specify the boundary condition that $u = u_B$ at $r = r_b$, which yields

$$n_b u_B = A(r_b - r_0)/r_b^2 \,. \tag{40}$$

Similarly, for $u = -u_B$ and $n = n_a$ at $r = r_a$, we obtain

$$-n_a u_B = A(r_a - r_0)/r_a^2 \,. \tag{41}$$

Eliminating r_0 from (40) and (41), we obtain

$$A = \frac{n_a r_a^2 + n_b r_b^2}{r_b - r_a}\, u_B \,. \tag{42}$$

Evaluating (39) at r_a and at r_b and subtracting the resulting two equations, we eliminate $n_{\max}$ to obtain

$$\frac{n_b^2 - n_a^2}{2} = \frac{\alpha A^2}{3r_0}\left[\left[\frac{r_0}{r_b} - 1\right]^3 + \left[\frac{r_0}{r_a} - 1\right]^3\right] . \tag{43}$$

Inserting (42) into (43) and introducing the normalized variables as in Sec. II, we obtain

$$\frac{N_b^2 - 1}{2} = \frac{D}{3\beta}\,\frac{\beta^3 - N_b^3}{\beta + N_b} \,, \tag{44}$$

where $D = \pi(r_b - r_a)/(2\lambda_i)$. The solution of (44) to first order in $1/D$ is

$$N_b \simeq [\beta^3 + 3\beta^2(1 - \beta^2)/D\,]^{1/3} \,. \tag{45}$$

For $D \gg 1$, (45) yields the ratio of densities at the grounded and powered electrodes

$$\frac{n_b}{n_a} \approx \beta = \left[\frac{A_a}{A_b}\right]^{1/2} . \tag{46}$$

Inserting (42) into (39), letting $n = n_a$ at $r = r_a$, and using (46), we also obtain

$$\frac{n_{\max}}{n_a} \approx (1+\beta D/3)^{1/2} . \tag{47}$$

These results are in good agreement with the results of Savas' ion transport code [21] for secondary electron ionization in the glow.

Inserting the density scaling (46) into (34), we obtain the area ratio scaling exponent $q = 2$. For Child's law sheaths, $q = 3$, while for Cobine's sheath law, $q = 2.5$. For a homogeneous sheath, $q = 1$. These values are shown in Table 1. Comparing these values to those for thermal electron ionization in the glow, we see that as secondary electron ionization increases in importance, the scaling exponent q (for a given sheath scaling law) is reduced.

VII. LOCAL IONIZATION NEAR THE SHEATHS

We consider the effect of local ionization near the sheaths due to stochastic heating[2,5,22-23] at the oscillating sheath-plasma boundaries. This heating mechanism is a powerful source of electron energy deposition in an r.f. discharge[22-24]. At high pressures, such that $s \le \lambda_e \ll d$, where λ_e is the mean free path for electrons having the ionization energy, there can be enhanced ionization near the sheath-plasma boundaries. Generally, this requires pressures exceeding 100 mTorr. Alternately, local ionization near the sheaths might be important at lower pressures if a significant population of metastable neutral atoms is present. In this case, the cross section for metastable ionization can be very large, such that $\lambda_e \ll d$ at relatively low pressures.

We let S be the power per unit area injected into the electrons by stochastic heating and $\mathcal{E}_c$ be the electron energy lost for each electron-ion pair created. For typical r.f. discharge parameters ($T_e \approx$ 3–5 eV in argon), $\mathcal{E}_c \approx$ 40–50 eV. Lieberman has obtained the scaling $S \propto V$ for both collisionless[22] and collisional[23] sheaths, independent of the electron density n_s at the sheath edge. Assuming that local ionization near each sheath dominates the overall ionization, we obtain from electron energy conservation the result that

$$S = en_s u_B \, e \mathcal{E}_c \ . \tag{48}$$

Since $S \propto V$, we obtain from (48) the scaling

$$n_a / n_b = V_a / V_b \ . \tag{49}$$

Combining (49), (32), and the constant mean free path sheath scaling (33), we obtain the area ratio scaling exponent $q = 5/4$. For Child's law sheath scaling, $q = 4/3$, while for Cobine's sheath law, $q = 3/2$. For a homogeneous sheath, $q = 1$. These values are shown in Table 1. We see that the effect of local ionization near the sheaths due to stochastic electron heating is to reduce the scaling exponent q from the value found for thermal ionization.

This work was supported by National Science Foundation Grant ECS-8517363 and Department of Energy Grant DE-FG03-87ER13727. Helpful discussions with S.E. Savas and A.J. Lichtenberg are gratefully acknowledged.

REFERENCES

1. H.R. Koenig and L.I. Maissel, *IBM J. Res. Dev.* **14**, 168 (1970).

2. J.L. Vossen, *J. Electrochem. Soc.* **126**, 2345 (1979).

3. J.H. Keller and W.P. Pennebaker, *IBM J. Res. Dev.* **23** 3 (1979).

4. J.A. Taillet, *J. Physique-Lettres* **40**, 223 (1979).

5. V.A. Godyak, *Sov. J. Plasma Phys.* **2**, 78 (1976).

6. V.A. Godyak and O. A. Popov, *Sov. J. Plasma Phys.* **5**, 227 (1979).

7. V.A. Godyak and Z. Kh. Ganna, *Sov. J. Plasma Phys.* **5**, 227 (1979).

8. V.A. Godyak and Z. Kh. Ganna, *Sov. J. Plasma Phys.* **6**, 372 (1980).

9. O.A. Popov and V.A. Godyak, *J. Appl. Phys.* **57**, 53 (1985).

10. V.A. Godyak and A.S. Khanneh, *IEEE Trans. Plasma Sci.* **PS-14**, 112 (1986).

11. V.A. Godyak, *Soviet Radio Frequency Discharge Research*, (Delphic Associates, Inc., Falls Church, VA), pp. 110-113 (1986).

12. B. Chapman, *Glow Discharge Processes*, Wiley, New York (1980).

13. J.W. Coburn and H.F. Winters, *J. Vac. Sci. Technol.* **16**, 391 (1979).

14. J.H. Keller, K. Kohler, J.W. Coburn, D.E. Horne, and E. Kay, *J. Appl. Phys.* **57**, 59 (1985).

15. J.W. Coburn and E. Kay, *J. Appl. Phys.* **43**, 4965 (1972).

16. C.M. Horwitz, *J. Vac. Sci. Technol. A* **1**, 60 (1983).

17. C.D. Child, *Phys. Rev.* **32**, 492 (1915).

18. J.D. Cobine, *Gaseous Conductors*, Dover, New York, p. 128 (1941).

19. Reference 5, p. 86.

20. S.E. Savas, *Mat. Res. Soc. Symp. Proc.* **98**, 35 (1987); 61 (1987).

21. S.E. Savas, private communication (1988).

22. M.A. Lieberman, *IEEE Trans. Plasma Sci.* **PS-16**, No. 6 (1988).

23. M.A. Lieberman, "Dynamics of a Collisional, Capacitive R.F. Sheath", Electronics Laboratory Report M88/62, College of Engineering, University of California, Berkeley, CA (1988); submitted to *IEEE Trans. Plasma Sci.*.

24. G.R. Misium, A.J. Lichtenberg, and M.A. Lieberman, "Macroscopic Modeling of R.F. Plasma Discharges", 35th National Symposium of the American Vacuum Society, Atlanta, GA, 3-7 October 1988; submitted to *J. Vac. Sci. Technol. A*.

25. G.R. Misium, "Modeling of RF Plasma Discharges for IC Processing", M. Eng. Thesis, College of Engineering, University of California, Berkeley, CA (1988).

	Sheath physics	Child's law	Cobine's law	Constant λ_i law	Homogeneous
Glow physics	Scaling law	$J \propto V^{3/2}/s^2$	$J \propto V^2/s^3$	$J \propto V^{3/2}/s^{5/2}$	$J \propto V/s^2$
Homogeneous	n=const	4.0	3.0	2.5	2.0
Thermal electron	$n \propto A^{-7/24}$	3.42	2.71	2.21	1.71
Secondary electron	$n \propto A^{-1/2}$	3.0	2.5	2.0	1.5
Local ionization	$n \propto V$	1.33	1.5	1.25	1.0

Table 1. Scaling exponent q for the dependence of the powered-to-grounded voltage ratio V_a/V_b on the area ratio A_b/A_a, where q is defined by $V_a/V_b = (A_b/A_a)^q$.

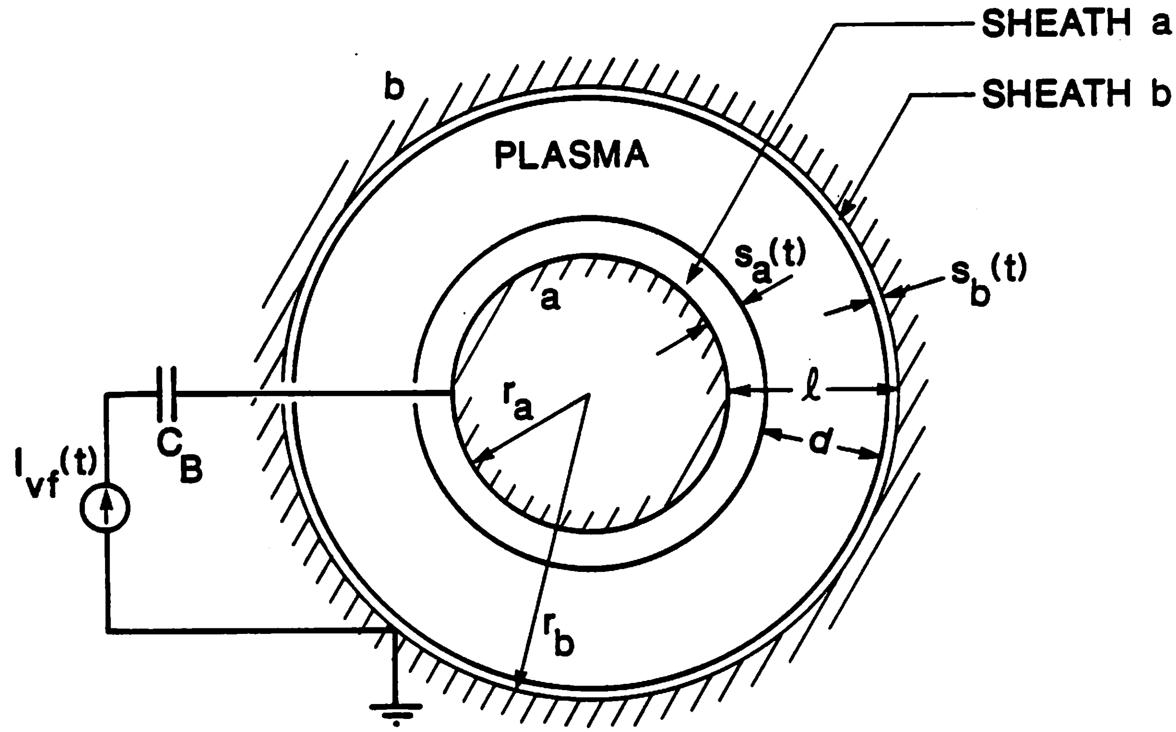

Fig. 1. Spherical shell model of an asymmetric r.f. discharge.

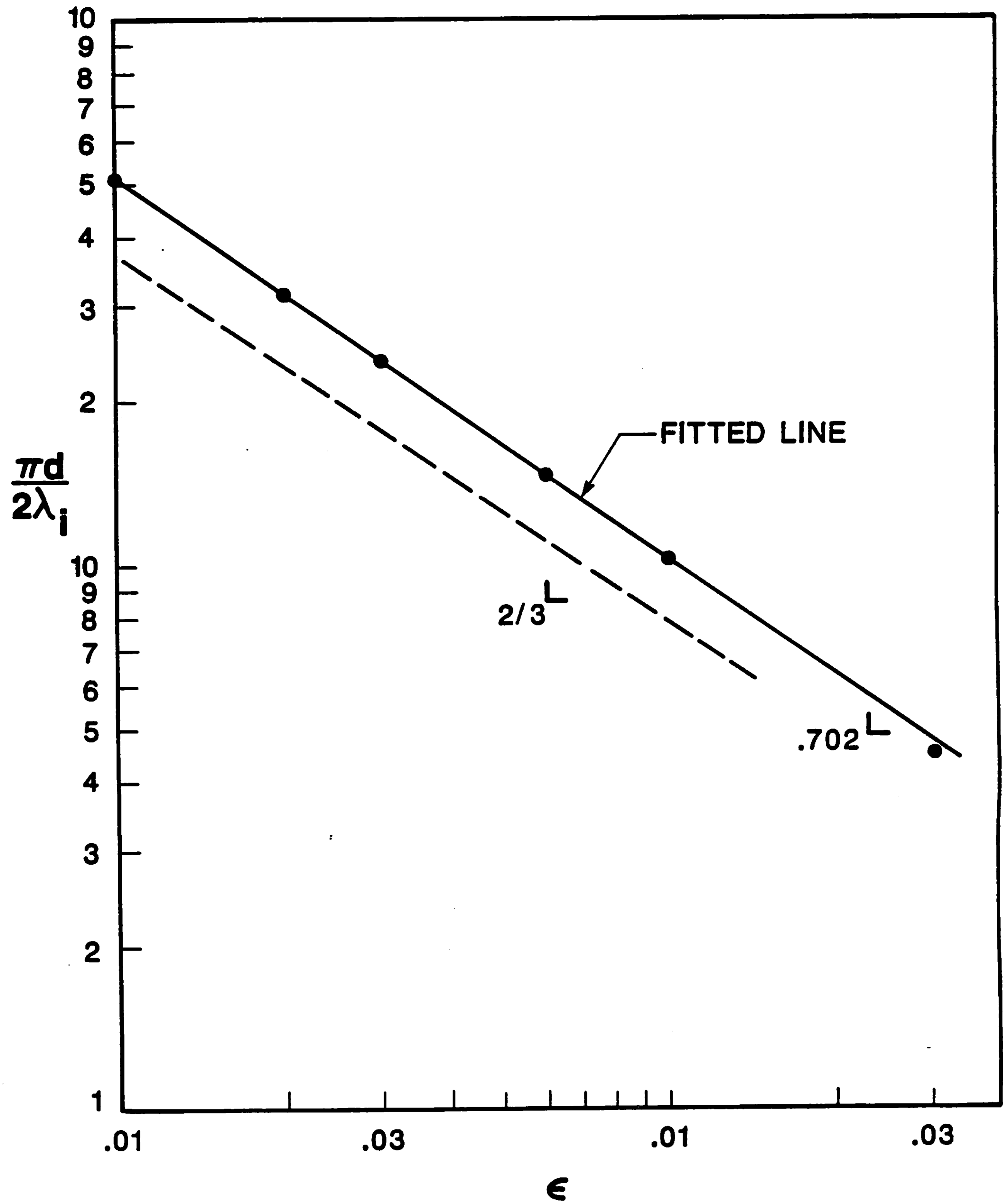

Fig. 2. The dependence of $\pi d/(2\lambda_i)$ on $\varepsilon = 2\lambda_i \nu_{iz}/(\pi u_B)$. The solid line gives the author's result, and the dashed line gives the approximate result of Godyak (see reference 19).

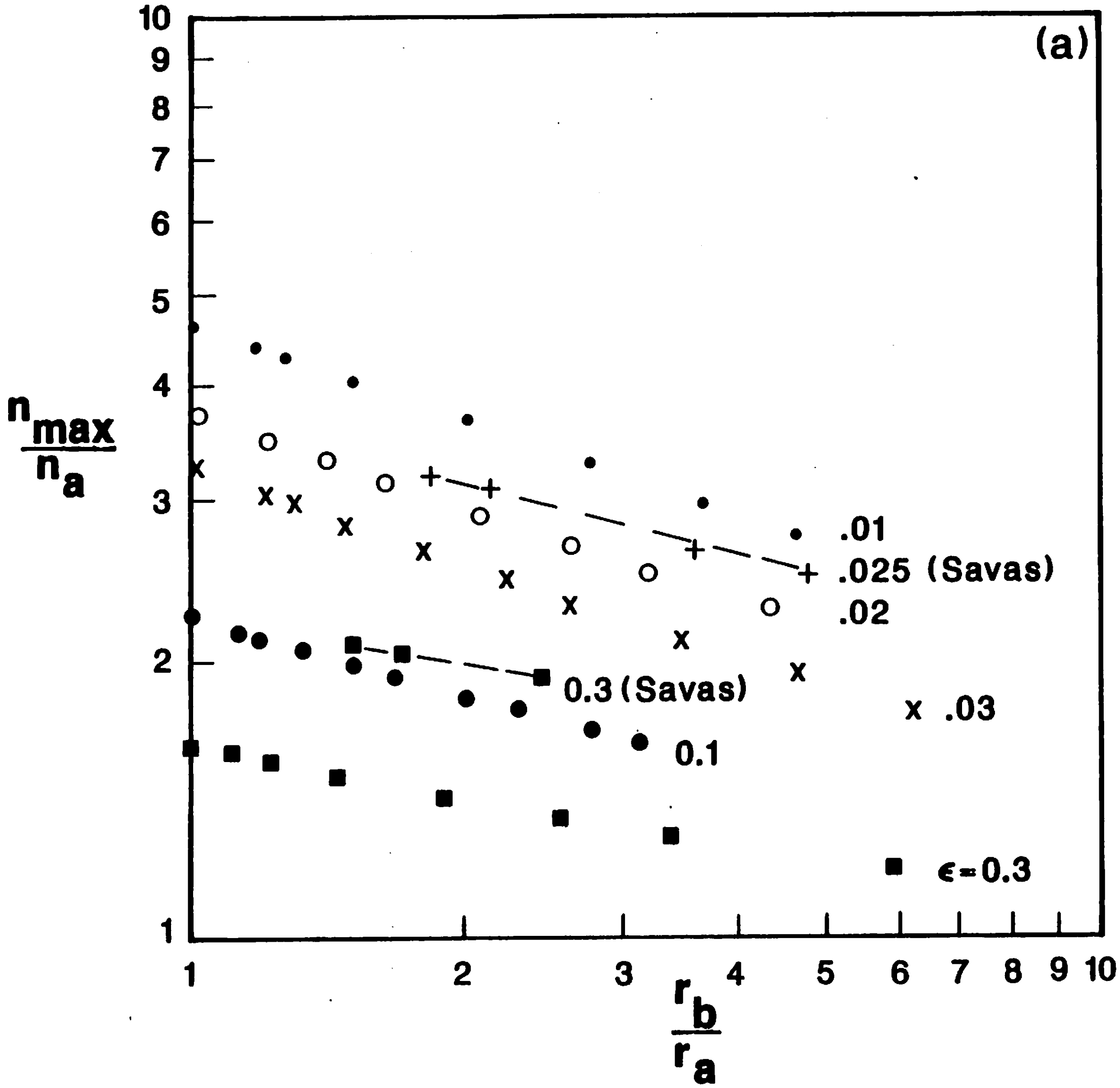

Fig. 3. The dependence of the density ratios (a) n_{max}/n_a, (b) n_{max}/n_b, and (c) n_b/n_a on $\beta^{-1} = r_b/r_a$ and ε.

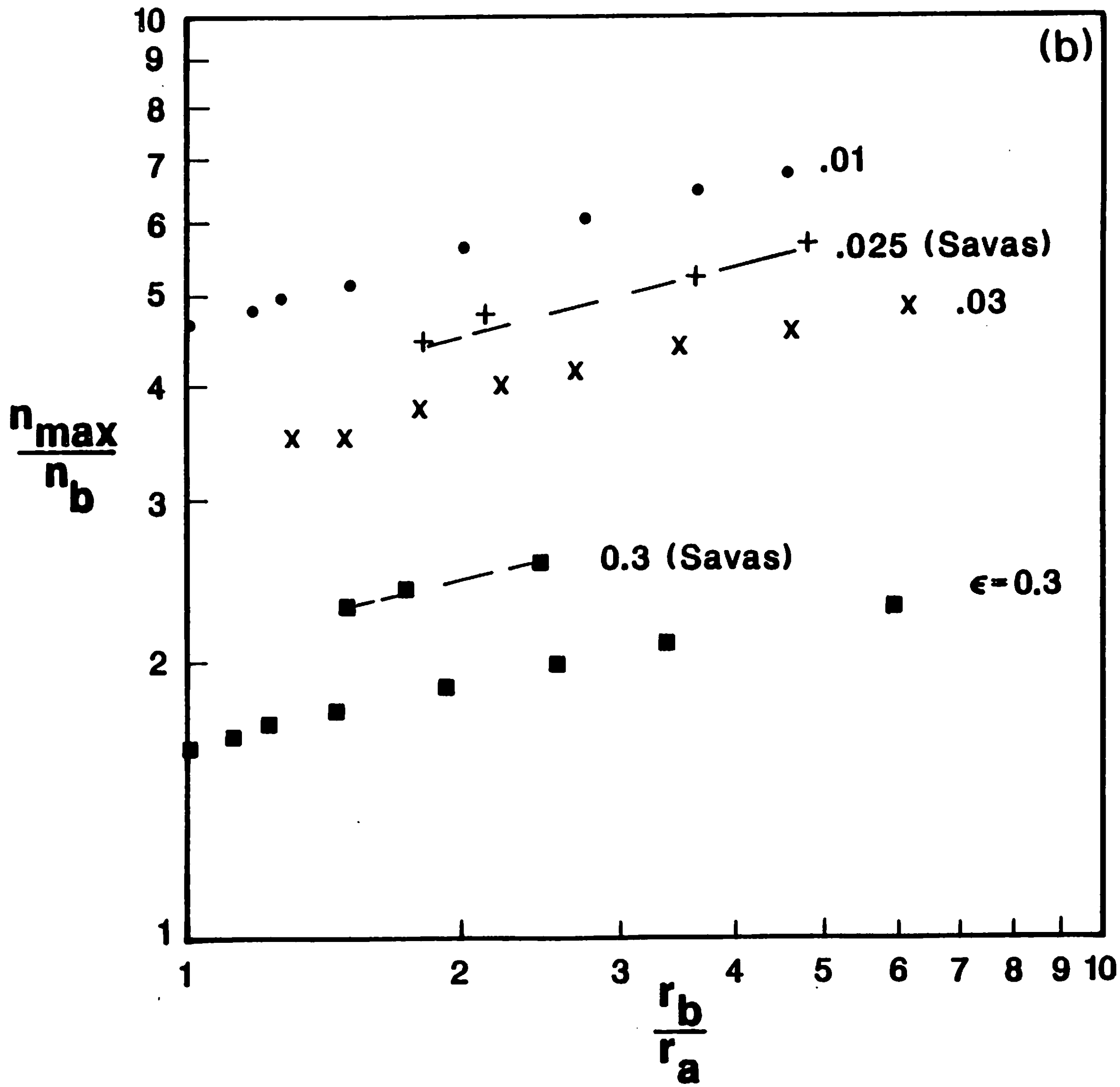
(b)
.01
.025 (Savas)
.03
0.3 (Savas)
ϵ=0.3
$\frac{n_{max}}{n_b}$
$\frac{r_b}{r_a}$
1
2
3
4
5
6
7
8
9
10

Fig. 3b

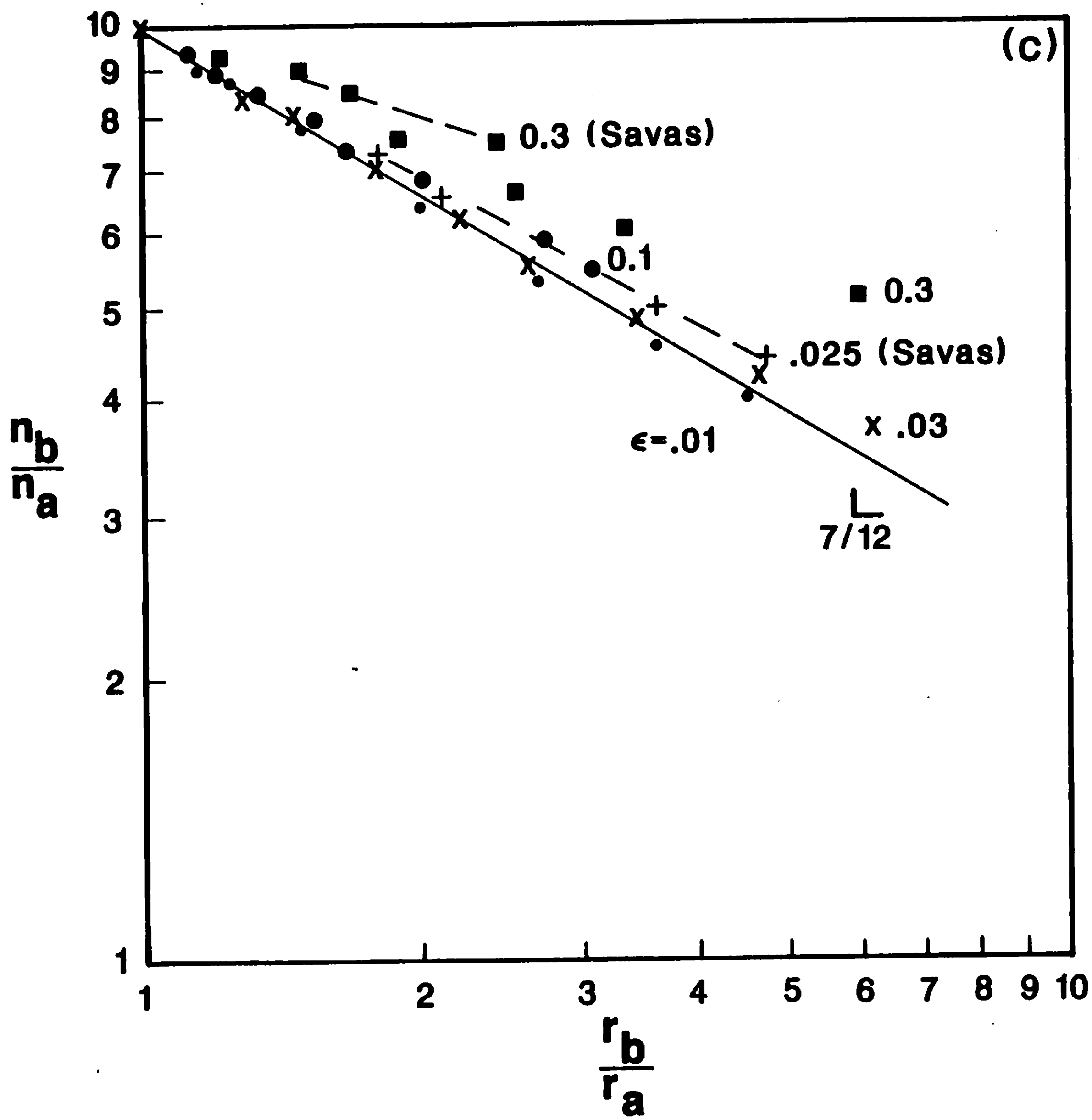

(c)
0.3 (Savas)
0.1
0.3
.025 (Savas)
x .03
ϵ=.01
7/12
10
9
8
7
6
5
4
3
2
1
1
2
3
4
5
6
7
8
9
10
$\frac{n_b}{n_a}$
$\frac{r_b}{r_a}$

Fig. 3c